AN INVESTIGATION OF THE STRUCTURE OF THE ACTIVE MASS OF THE NEGATIVE PLATE OF LEAD–ACID BATTERIES

D. PAVLOV and V. ILIEV

Central Laboratory of Electrochemical Power Sources, Bulgarian Academy of Sciences, 1040 Sofia (Bulgaria)

Summary

The formation of the negative plate of the lead–acid battery has been shown to take place in two stages. During the first stage, lead monoxide and basic lead sulphates are partially reduced to lead and partially react with H_2SO_4 to give $PbSO_4$. These processes proceed at a neutral pH. SEM micrographs show that the lead crystals are interlinked in a skeletal primary network and that the $PbSO_4$ crystals form on the surface of this structure. During the second stage, $PbSO_4$ is reduced to lead under acidic conditions. Lead crystals are precipitated on the lead skeleton and form a secondary structure different from that of the primary skeleton. Upon discharge, current is generated mainly at the expense of the oxidation of the secondary structure lead crystals. The functions of the two types of structures have been identified. The primary (skeleton) structure serves as both a current collector and a mechanical support of the lead obtained during the second stage. The secondary (energetic) structure participates mainly in the charge–discharge processes of the negative plate.

Introduction

It is well known that both the capacity and the cycle life of lead–acid batteries are dependent on the conditions of plate formation. For example, Steffans [1] has shown that whereas formation in 1.24 sp.gr H_2SO_4 results in a high initial capacity but short cycle life, the use of 1.06 sp.gr. acid has the converse effect; namely, low initial capacity and long cycle life. Findings such as these indicate that the plates gain a "memory" during formation. This memory effect lasts for many charge–discharge cycles but it appears that during operation of the battery the "genetic code" initially created upon formation is eventually destroyed. If the battery is considered as an energy system with its own structure, the process of degradation of its characteristics may be envisaged as a disintegration of this structure.

The aim of the present investigation was (a) to identify the structures created during formation of the active mass of the negative plate and (b) to establish the roles these structures may play during battery operation.

Experimental

Plates of 12 A h capacity were prepared with a paste containing 4.5 wt.% H_2SO_4 (with regard to the weight of lead oxide), 0.4% $BaSO_4$, 0.25% carbon black, and 0.4% lignin sulphonate. After curing for 72 h the plates were formed for 20 h at a current density of 5 mA/cm^2 in an H_2SO_4 solution of sp. gr. 1.05. Specimens were taken from the plates every 2 h and analysed for phase composition (by X-ray diffraction), cross-sectional distribution of formed and unformed zones (under a binocular microscope), and crystal microstructure of formed zones (by scanning electron microscopy). The method for phase composition studies of the plates is given in ref. 2.
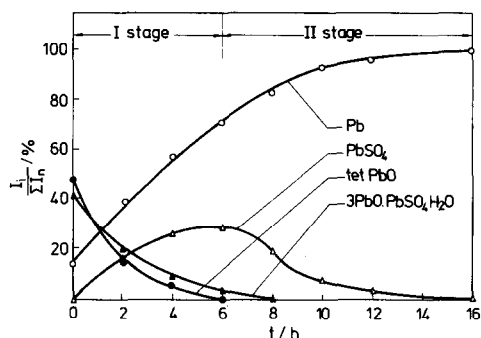

Fig. 1. Change in the phase composition during formation.

Processes involved in the formation of the negative plate

Figure 1 illustrates the change in the phase composition during formation of the negative plate. The relative intensities of the diagnostic X-ray diffraction lines are plotted on the ordinate. It is seen that formation occurs in two successive stages. Initially tet-PbO and $3PbO.PbSO_4 \cdot H_2O$ are both reduced, in part, to lead, and converted to $PbSO_4$ through reaction with H_2SO_4. In the second stage of formation the $PbSO_4$ already formed is reduced to lead. This two-stage formation of the active lead mass has been established previously by Pavlov *et al.* [2] who suggested that the formation of Pb from a paste containing $3PbO.PbSO_4 \cdot H_2O$ and PbO takes place *via* electrochemical and chemical reactions proceeding in a reaction layer located between the paste and the formed zone of Pb and $PbSO_4$. A general reaction scheme which includes lead oxide and all the basic lead sulphates is shown in Fig. 2. This scheme gives only the stoichiometry of the reactions taking place
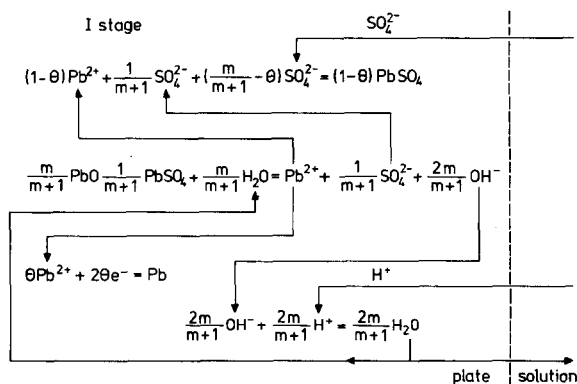
I stage SO_4^{2-}

$(1-\theta)Pb^{2+} + \dfrac{1}{m+1}SO_4^{2-} + (\dfrac{m}{m+1} - \theta)SO_4^{2-} = (1-\theta)PbSO_4$

$\dfrac{m}{m+1}PbO - \dfrac{1}{m+1}PbSO_4 + \dfrac{m}{m+1}H_2O = Pb^{2+} + \dfrac{1}{m+1}SO_4^{2-} + \dfrac{2m}{m+1}OH^-$

$\theta Pb^{2+} + 2\theta e^- = Pb$ $\qquad\qquad$ H^+

$\dfrac{2m}{m+1}OH^- + \dfrac{2m}{m+1}H^+ = \dfrac{2m}{m+1}H_2O$

plate $\mid$ solution

Fig. 2. Diagram of the chemical and electrochemical reactions (with the corresponding stoichiometric coefficients of the compounds) during the first stage of formation.

during the first stage and not the elementary processes. The coefficient m takes into account the "PbO molecules" in the basic lead sulphates; when $m = \infty$ the corresponding numerial values of PbO and $PbSO_4$ in the general formula are unity for PbO and zero for $PbSO_4$, i.e., only PbO is present. When $m = 3$ the paste consists of $3PbO.PbSO_4 \cdot H_2O$ and at $m = 1$ the paste is constituted by $PbO.PbSO_4$.

An exchange of H^+ and SO_4^{2-} ions and H_2O molecules has to occur between the reaction layer and the bulk of the electrolyte for the reactions to proceed. The quantity θ is that portion of the Pb^{2+} ions which participates in the electrochemical reaction.

II stage

$SO_4^{2-} + 2H^+ \longrightarrow H_2SO_4$

$PbSO_4 \rightleftharpoons Pb^{2+} + SO_4^{2-}$

$Pb^{2+} + 2e^- \longrightarrow Pb$
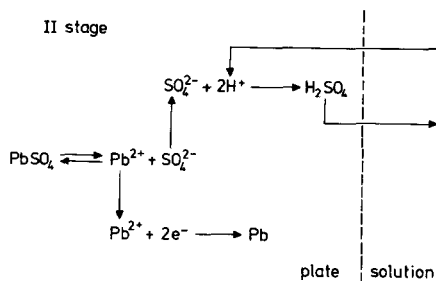
plate $\mid$ solution

Fig. 3. Diagram of the reactions during the second stage of formation of the negative plate.

Figure 3 shows the reaction scheme during the second stage of formation. By considering the elementary physicochemical diffusion and migration processes Pavlov [3] deduced that the second stage commences in a second reaction layer before the end of the first stage of formation. This second reaction layer is at a distance from that in which the reactions of the first stage take place.

From a comparison of the reaction schemes shown in Figs. 2 and 3 it becomes clear that during the two stages the growth of lead crystals takes place at different pHs. During the first stage, the solution in the reaction layer is neutral (since water is formed). However, the production of H_2SO_4 during the second period gives rise to a strongly acidic medium. The lead structures formed in the two successive stages are termed primary and secondary structures, respectively. It is assumed that the morphology of the lead crystals of the primary and secondary structures are different.

Zonal processes and morphology of the crystals formed during formation of negative plates

Figure 4 presents micrographs of the cross-section of a plate during formation. It is seen that the formation of lead begins first at those portions of the grid members that are closest to the solution. The electrochemical and chemical reactions lead to the appearance of a zone which consists, according to X-ray diffraction analysis, of Pb and $PbSO_4$ crystals. The Pb–$PbSO_4$ zone (dark zones in the plate cross section) advances first along the surface layers of the plate and then into the interior. After the Pb–$PbSO_4$ zone has occupied almost the entire cross section of the plate reduction of $PbSO_4$ to Pb begins. Since the latter process does not bring about drastic colour changes it is not possible to follow the second stage of the formation by optical techniques. The development of the Pb–$PbSO_4$ zone has been reported by other workers [2, 4 - 6].

It is of interest to consider the morphology of the crystals in the Pb–$PbSO_4$ zone. Figure 5 presents a SEM micrograph of the crystal structure of the zone; $PbSO_4$ crystals with different morphologies can be seen.

In order to establish the microstructure of the Pb crystals in the Pb–$PbSO_4$ zone, part of the plate was immersed in a boiling, saturated solution of ammonium acetate for $\frac{1}{2}$ h. The remaining undissolved portion of the sample was washed with water and dried under a nitrogen atmosphere. This treatment dissolves all divalent lead compounds but leaves lead itself unaffected. The structure of the residual lead sample was subjected to SEM examination. Figure 6 represents a micrograph of the primary lead crystal structure which is produced during the first stage of formation. The structure consists of a skeleton of interlinked crystals of irregular shape. The length and thickness of the individual branches range from 3 to 10 μm and from 2 to 5 μm, respectively. If we compare Figs. 5 and 6 it becomes clear that the Pb–$PbSO_4$ zone formed during the first stage consists of a skeleton of lead covered by $PbSO_4$ crystals.

The lead microstructure of a completely formed plate is shown in Fig. 7. Small isolated lead crystals developed from the $PbSO_4$ during the second stage of formation can be seen. These crystals are located on the lead skeleton formed during the first stage and represent the secondary structure. Thus the negative active material consists of a network of interlinked crystals covered by smaller secondary lead crystals.
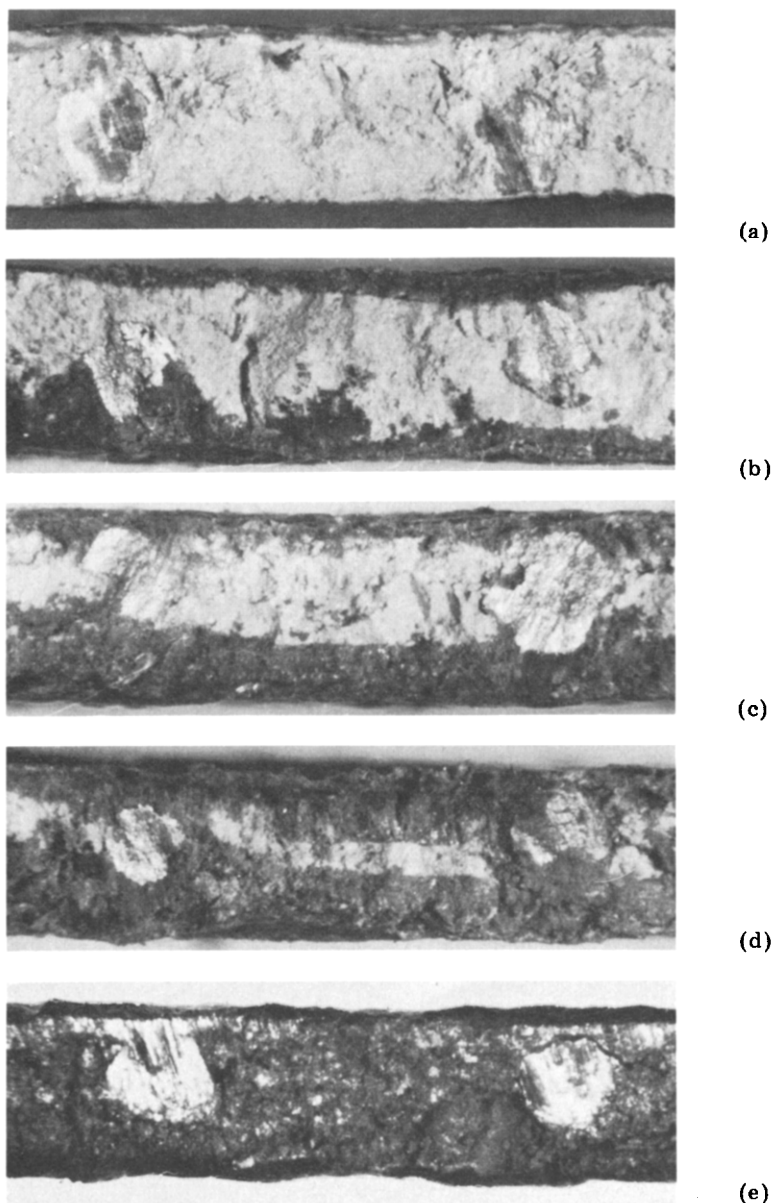
Fig. 4. Micrograph of the cross section of the negative plate during formation. (a) Prior to formation; (b) - (d) during formation. The dark portions are the Pb–PbSO$_4$ zone; (e) completely formed plate.

The existence of two types of lead crystals in the negative plate active material has been recognised in earlier studies. For example, Willihnganz [7] and Simon and Jones [4] have found that the negative active mass consists of acicular and rounded crystals which depend on the conditions of formation.
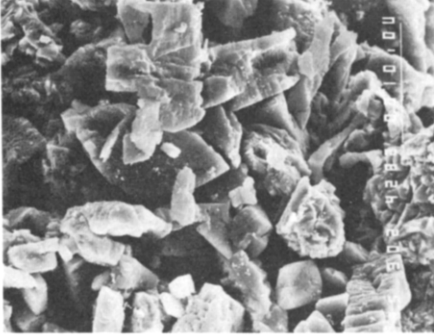
Fig. 5 (left). SEM micrograph of the crystals in the Pb–PbSO$_4$ zone during the first stage of formation of the negative plate. Magnification × 3000.
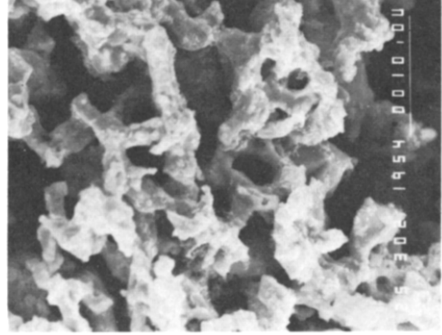
Fig. 6 (right). SEM micrograph of the Pb crystal skeleton during the first stage of formation of negative plates. Magnification × 3000.
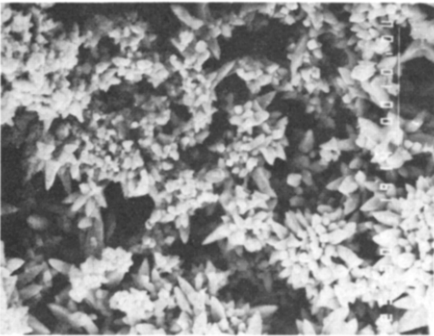

Fig. 7. SEM micrograph of Pb crystals in a completely formed negative plate. Magnification × 3000.

Studies using SEM and optical microscopy of lead crystals in formed and cycled negative plates have revealed a diversity of crystal morphologies [8 - 12]. It is considered that this is due to the influence of expanders as well as to the conditions of formation.

Having identified the processes which lead to the appearance of the different microstructures during plate formation it remains to consider their role during subsequent operation of the battery.

Role of the negative plate microstructures during battery operation

Negative plates formed under the conditions described above were combined with two positive plates in individual cells and subjected to constant current charge–discharge cycles, charging at $i = 5$ mA/cm^2 and discharging at
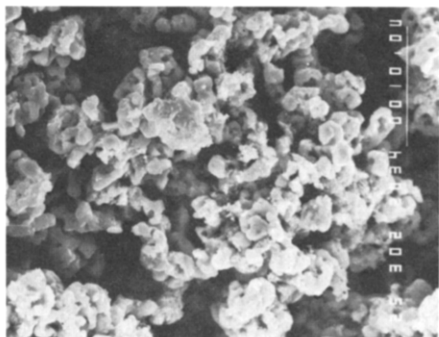
Fig. 8 (left). SEM micrograph of lead crystals in a completely charged negative plate after 10 charge—discharge cycles. Magnification × 3000.
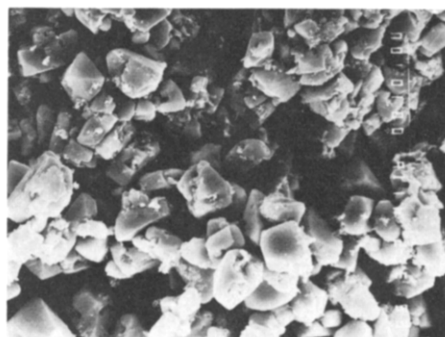
Fig. 9 (right). SEM micrograph of the crystals of a completely discharged negative plate after 10 charge—discharge cycles. Magnification × 3000.

the same current density to a potential of − 600 mV (*vs.* Hg/Hg_2SO_4 electrode).

    Lead crystals in a charged plate after 10 such cycles are shown in Fig. 8. A comparison of Figs. 7 and 8 shows that the general shape of the lead crystals after cycling is different from that after formation. This is to be expected since the charge—discharge processes in the negative plate take place *via* a dissolution—precipitation mechanism [11].

    After completion of 10 cycles the cell was discharged for about 10 h. The negative plate was then removed and washed and dried under a nitrogen atmosphere. Samples of the active mass were taken and the morphology of the crystals examined. Densely packed $PbSO_4$ crystals ranging in size from 1 to 4 μm were identified (Fig. 9).

    In order to study the morphologies of the underlying lead crystals, $PbSO_4$ was dissolved from the plate using the ammonium acetate method described above. An electron micrograph of the lead substructure is shown in Fig. 10. By comparison with Fig. 6 it can be seen that the lead structure formed during the first stage of plate preparation has been left virtually unaffected by the charge—discharge cycling. It is therefore concluded that this lead skeleton has a dual purpose, *i.e.*, it serves as both a current collector for all parts of the plate and as a mechanical support for the active part of the lead which participates in current generation.

    By comparing Figs. 9 and 10 it becomes obvious that the plate ceases to generate current when the skeleton is covered by a dense layer of $PbSO_4$ crystals. We therefore conclude that the capacity of the negative plate is determined mainly by the secondary lead structure. Since secondary lead formation involves dissolved lead ions, the morphology of the secondary lead structure will be a function of the operating conditions of the battery.

    In order to confirm the above conclusions the amounts of lead in the plate produced during the first and the second stages of formation as well as
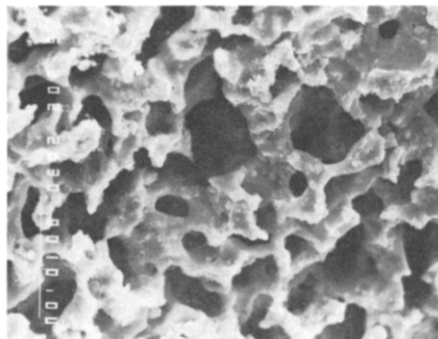
Fig. 10. SEM micrograph of a completely discharged negative plate after dissolution of the PbSO$_4$ crystals. A skeleton structure similar to that in Fig. 6 is apparent. Magnification × 3000.

the amount of lead oxidized upon discharge of the plate, were determined by complexometry. Table 1 presents these data in terms of the equivalent quantity of electricity. It can be seen that the capacity is equivalent to the total discharge of the secondary lead structure together with a 10 - 15% discharge of the lead skeleton. On this basis it is reasonable to conclude that the secondary structure participates mainly in the processes of current generation. Thus we choose to term this structure "energetic".

TABLE 1

Stage	Experimentally determined amount of Pb during formation		Experimentally determined capacity upon discharge (A h/plate)
	g/plate	A h/plate	
First	46	11.9	
Second	45	11.6	
Total per plate	91	23.5	13.5

## Effect of production technology on the negative plate structure

In order to assess to what extent this structure is typical, negative plates produced by three different companies were studied: BALKANCAR (Bulgaria), VARTA (FRG), and DELCO (USA). The BALKANCAR and VARTA plates used lead–antimony alloy grids whereas the DELCO ones employed expanded lead–calcium technology. Figure 11 shows micrographs of lead crystals after the initial charge for 15 h with i = 14 mA/g.a.m. (gram
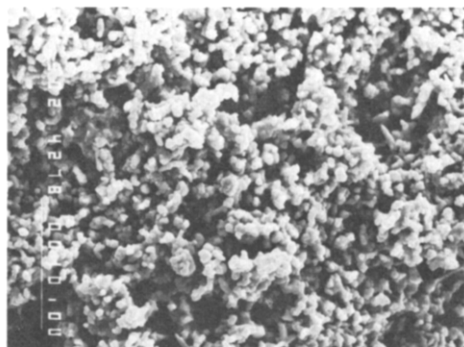
(a)
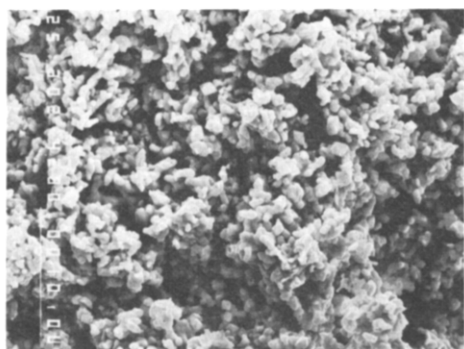
(b)
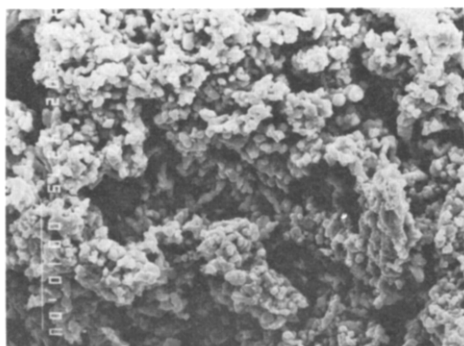
(c)

Fig. 11. SEM micrograph of completely charged negative plates during the initial cycle. (a) DELCO, (b) VARTA and (c) BALKANCAR plates. Magnification × 3000.

active mass) of new batteries. There is no essential difference between the lead crystals formed in the three types of plates.

The batteries were then discharged at a constant current of $i = 4 \text{ mA/cm}^2$ down to a potential of -600 mV. The morphology of the $PbSO_4$ crystals thus obtained is not dependent on the origin of the plates, Fig. 12. Treatment with an ammonium acetate solution reveals the presence of a lead skeleton in the plates of each make of battery, Fig. 13. Therefore, irrespective of the production technology, the negative plates consist of two types of structure: primary (skeleton) and secondary (energetic).
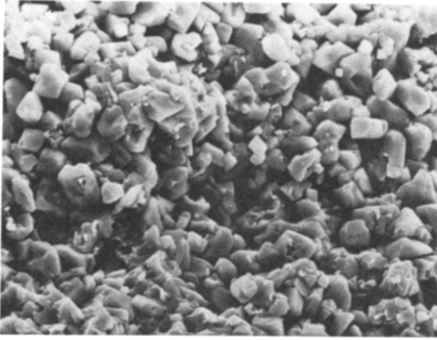
(a)
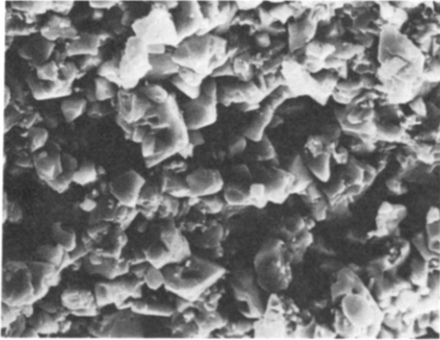
(b)
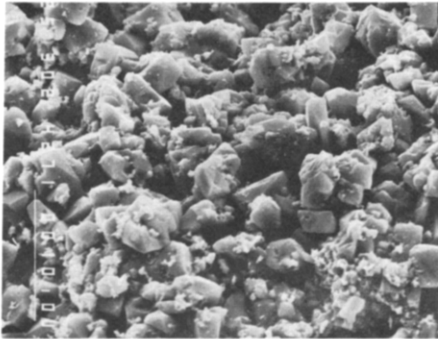
(c)

Fig. 12. SEM micrograph of PbSO$_4$ crystals of completely discharged negative plates produced by (a) DELCO, (b) VARTA and (c) BALKANCAR. Magnifica-

Figure 13 further shows that the skeleton structure is very different in the three types of plates. This means that the primary structure is strongly affected by the production technology of the negative plate, *e.g.*, phase composition and density of the paste, nature and amount of expander, concentration of the formation electrolyte, current density and temperature of the formation, etc.
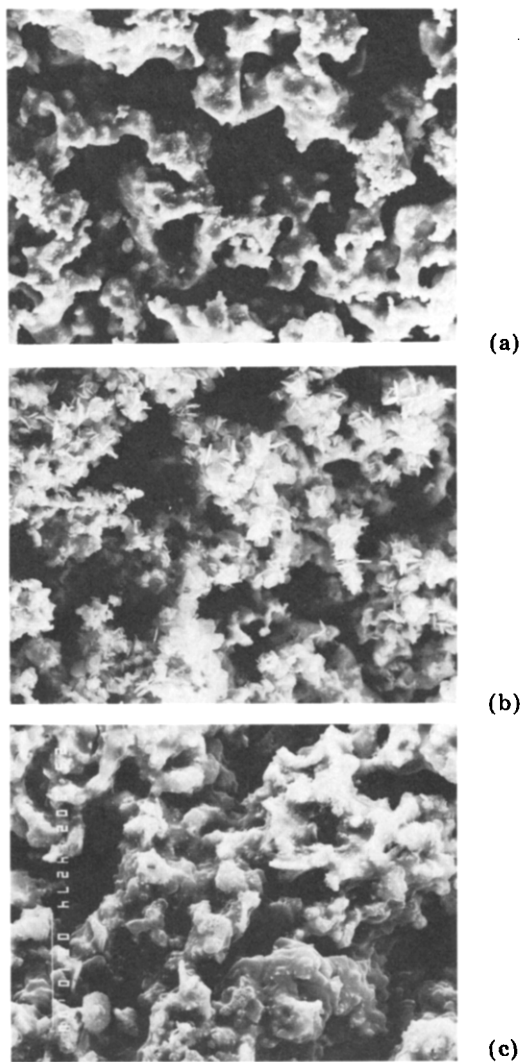
Fig. 13. SEM micrographs of the primary (skeleton) structure after discharge of negative plates produced by (a) DELCO, (b) VARTA and (c) BALKANCAR. Magnification × 3000.

Conclusion

During pasting of the grids the paste is homogeneous in all parts of the plate. However, during formation the electrochemical processes proceed in two stages and in two different layers of the cross-section [3]. Different initial products are reduced during these processes. Microheterogeneity is thus created by the appearance of a primary and of a secondary structure. During operation of the battery (charge–discharge cycles) these two

structures play different roles. It may be expected that both the energetic parameters (*i.e.*, capacity, power) and cycle life of the plate will depend on the relative proportions of these structures. The preservation of an optimum ratio between these two structures will determine the stability of the operating parameters of the negative plate of the battery. Wide variations in this ratio will lead to failure of the battery.

The secondary structure of the negative plate appears and disappears at each charge–discharge cycle. On the other hand, the skeleton structure changes slowly during the cycle life of the battery. Therefore the primary structure created during the first stage of formation constitutes the "memory".

Acknowledgements

References

1 F. Steffans, Paper 61, *156th Meeting of the Electrochemical Society, Los Angeles, California, October 14, 1979*.
2 D. Pavlov, V. Iliev, G. Papazov and E. Bashtavelova, *J. Electrochem. Soc., 121* (1974) 854.
3 D. Pavlov, *J. Electroanal. Chem., 72* (1976) 319.
4 A. C. Simon and E. L. Jones, *J. Electrochem. Soc., 109* (1962) 760.
5 N. E. Bagshaw and K. P. Willson, *Electrochim. Acta., 10* (1965) 867.
6 D. Pavlov and G. Papazov, *J. Electrochem. Soc., 127* (1980) 2104.
7 E. Willihnganz, *Spring Meeting of the National Battery Manufacturers Association, White Sulphur Springs, W.VA, May, 1940*.
8 A. C. Simon, in D. H. Collins (ed.), *Power Sources 2*, Pergamon Press, New York, 1968, p. 33.
9 J. R. Pierson, P. Gurlusky, A. C. Simon and S. M. Caulder, *J. Electrochem. Soc., 117* (1970) 1463.
10 T. Y. Hughel and R. H. Hammar, in D. H. Collins (ed.), *Power Sources 3*, Oriel Press, Newcastle Upon Tyne, England, 1971, p. 35.
11 J. W. Weininger, *J. Electrochem. Soc., 121* (1974) 1454.
12 S. Hattori, M. Yamura, M. Kohno, Y. Ohtani, M. Yamane and H. Nakashima, in D. H. Collins (ed.), *Power Sources 5*, Academic Press, New York, 1975, p. 139.